Measurement of branching fractions and charge asymmetries for two-body *B* meson decays with charmonium

K. Abe,[6] R. Abe,[25] T. Abe,[39] I. Adachi,[6] H. Aihara,[40] M. Akatsu,[19] Y. Asano,[45] T. Aso,[44] T. Aushev,[9] A. M. Bakich,[35] Y. Ban,[29] A. Bay,[15] P. K. Behera,[46] I. Bizjak,[10] A. Bondar,[1] A. Bozek,[23] M. Bračko,[17,10] J. Brodzicka,[23] T. E. Browder,[5] B. C. K. Casey,[5] P. Chang,[22] Y. Chao,[22] K.-F. Chen,[22] B. G. Cheon,[34] R. Chistov,[9] S.-K. Choi,[4] Y. Choi,[34] M. Danilov,[9] L. Y. Dong,[7] J. Dragic,[18] A. Drutskoy,[9] S. Eidelman,[1] V. Eiges,[9] C. Fukunaga,[42] N. Gabyshev,[6] A. Garmash,[1,6] T. Gershon,[6] B. Golob,[16,10] A. Gordon,[18] J. Haba,[6] N. C. Hastings,[18] M. Hazumi,[6] I. Higuchi,[39] L. Hinz,[15] T. Hojo,[27] T. Hokuue,[19] Y. Hoshi,[38] W.-S. Hou,[22] H.-C. Huang,[22] T. Iijima,[19] K. Inami,[19] A. Ishikawa,[19] R. Itoh,[6] H. Iwasaki,[6] Y. Iwasaki,[6] H. K. Jang,[33] J. H. Kang,[49] J. S. Kang,[12] P. Kapusta,[23] S. U. Kataoka,[20] N. Katayama,[6] H. Kawai,[40] Y. Kawakami,[19] T. Kawasaki,[25] H. Kichimi,[6] D. W. Kim,[34] H. J. Kim,[49] H. O. Kim,[34] Hyunwoo Kim,[12] S. K. Kim,[33] K. Kinoshita,[3] S. Kobayashi,[31] S. Korpar,[17,10] P. Križan,[16,10] P. Krokovny,[1] R. Kulasiri,[3] S. Kumar,[28] Y.-J. Kwon,[49] G. Leder,[8] S. H. Lee,[33] J. Li,[32] D. Liventsev,[9] R.-S. Lu,[22] J. MacNaughton,[8] G. Majumder,[36] F. Mandl,[8] D. Marlow,[30] S. Matsumoto,[2] T. Matsumoto,[42] W. Mitaroff,[8] K. Miyabayashi,[20] H. Miyata,[25] T. Mori,[2] T. Nagamine,[39] T. Nakadaira,[40] E. Nakano,[26] H. Nakazawa,[6] J. W. Nam,[34] Z. Natkaniec,[23] S. Nishida,[13] O. Nitoh,[43] S. Noguchi,[20] T. Nozaki,[6] S. Ogawa,[37] T. Ohshima,[19] T. Okabe,[19] S. Okuno,[11] S. L. Olsen,[5] Y. Onuki,[25] W. Ostrowicz,[23] H. Ozaki,[6] P. Pakhlov,[9] H. Palka,[23] C. W. Park,[12] H. Park,[14] M. Peters,[5] L. E. Piilonen,[47] F. J. Ronga,[15] K. Rybicki,[23] H. Sagawa,[6] S. Saitoh,[6] Y. Sakai,[6] M. Satapathy,[46] A. Satpathy,[6,3] O. Schneider,[15] S. Schrenk,[3] C. Schwanda,[6,8] S. Semenov,[9] K. Senyo,[19] R. Seuster,[5] H. Shibuya,[37] V. Sidorov,[1] J. B. Singh,[28] N. Soni,[28] S. Stanič,[45,*] M. Starič,[10] A. Sugi,[19] K. Sumisawa,[6] T. Sumiyoshi,[42] S. Suzuki,[48] S. Y. Suzuki,[6] T. Takahashi,[26] F. Takasaki,[6] K. Tamai,[6] N. Tamura,[25] J. Tanaka,[40] M. Tanaka,[6] G. N. Taylor,[18] Y. Teramoto,[26] T. Tomura,[40] T. Tsuboyama,[6] T. Tsukamoto,[6] S. Uehara,[6] S. Uno,[6] G. Varner,[5] K. E. Varvell,[35] C. C. Wang,[22] C. H. Wang,[21] J. G. Wang,[47] M.-Z. Wang,[22] Y. Watanabe,[41] E. Won,[12] B. D. Yabsley,[47] Y. Yamada,[6] A. Yamaguchi,[39] Y. Yamashita,[24] H. Yanai,[25] M. Yokoyama,[40] Y. Yuan,[7] Z. P. Zhang,[32] and D. Žontar[45]

(Belle Collaboration)

[1]*Budker Institute of Nuclear Physics, Novosibirsk*
[2]*Chuo University, Tokyo*
[3]*University of Cincinnati, Cincinnati, Ohio 45221*
[4]*Gyeongsang National University, Chinju*
[5]*University of Hawaii, Honolulu, Hawaii 96822*
[6]*High Energy Accelerator Research Organization (KEK), Tsukuba*
[7]*Institute of High Energy Physics, Chinese Academy of Sciences, Beijing*
[8]*Institute of High Energy Physics, Vienna*
[9]*Institute for Theoretical and Experimental Physics, Moscow*
[10]*J. Stefan Institute, Ljubljana*
[11]*Kanagawa University, Yokohama*
[12]*Korea University, Seoul*
[13]*Kyoto University, Kyoto*
[14]*Kyungpook National University, Taegu*
[15]*Institut de Physique des Hautes Énergies, Université de Lausanne, Lausanne*
[16]*University of Ljubljana, Ljubljana*
[17]*University of Maribor, Maribor*
[18]*University of Melbourne, Victoria*
[19]*Nagoya University, Nagoya*
[20]*Nara Women's University, Nara*
[21]*National Lien-Ho Institute of Technology, Miao Li*
[22]*National Taiwan University, Taipei*
[23]*H. Niewodniczanski Institute of Nuclear Physics, Krakow*
[24]*Nihon Dental College, Niigata*
[25]*Niigata University, Niigata*
[26]*Osaka City University, Osaka*
[27]*Osaka University, Osaka*
[28]*Panjab University, Chandigarh*
[29]*Peking University, Beijing*
[30]*Princeton University, Princeton, New Jersey 08545*

---

*On leave from Nova Gorica Polytechnic, Nova Gorica.

67 032003-1

^{31}*Saga University, Saga*

^{32}*University of Science and Technology of China, Hefei*

^{33}*Seoul National University, Seoul*

^{34}*Sungkyunkwan University, Suwon*

^{35}*University of Sydney, Sydney NSW*

^{36}*Tata Institute of Fundamental Research, Bombay*

^{37}*Toho University, Funabashi*

^{38}*Tohoku Gakuin University, Tagajo*

^{39}*Tohoku University, Sendai*

^{40}*University of Tokyo, Tokyo*

^{41}*Tokyo Institute of Technology, Tokyo*

^{42}*Tokyo Metropolitan University, Tokyo*

^{43}*Tokyo University of Agriculture and Technology, Tokyo*

^{44}*Toyama National College of Maritime Technology, Toyama*

^{45}*University of Tsukuba, Tsukuba*

^{46}*Utkal University, Bhubaneswer*

^{47}*Virginia Polytechnic Institute and State University, Blacksburg, Virginia 24061*

^{48}*Yokkaichi University, Yokkaichi*

^{49}*Yonsei University, Seoul*

We report branching fractions and charge asymmetries for exclusive decays of charged and neutral B mesons to two-body final states containing a charmonium meson, J/ψ or $\psi(2S)$. This result is based on a 29.4 fb^{-1} data sample collected at the $\Upsilon(4S)$ resonance with the Belle detector at the KEKB asymmetric e^+e^- collider.

I. INTRODUCTION

Investigation of CP violation is one of the key issues facing elementary particle physics. Recently, the BaBar [1] and Belle [2] Collaborations have observed large time-dependent CP asymmetries in the neutral B-meson system [3]. Decay modes of neutral B mesons to final states containing charmonia were used for these measurements due to their clean experimental signatures and straightforward theoretical interpretation. It is expected for the same reasons that exclusive charmonium modes will continue to play a major role in CP studies, with rarer modes contributing as the body of data grows in magnitude and different aspects of the CP question move to the forefront. For example, the Kobayashi-Maskawa model [4] predicts small direct CP violation for $B \rightarrow J/\psi K^\pm$ and $B \rightarrow J/\psi \pi^\pm$ [5]. Large direct CP violation would indicate new physics [6]. In addition, the dominant mechanism for charmonium production in B-meson decay is color suppressed, so precise measurements of rates to the exclusive modes can provide important information toward the understanding of color suppression.

In this paper we report measurements of branching fractions and charge asymmetries for the exclusive decays of B mesons to the two-body final states ψh, where ψ is J/ψ or $\psi(2S)$ and h is one of the light mesons $K^\pm$, K_S^0, $\pi^\pm$, or π^0. We used a 29.4 fb^{-1} data set which contains 31.9 million $B\bar{B}$ events collected with the Belle detector [8] at KEKB [9].

II. THE BELLE DETECTOR

KEKB is an asymmetric electron-positron storage ring that collides 8.0 GeV electrons with 3.5 GeV positrons at the $\Upsilon(4S)$ resonance (10.58 GeV center-of-mass energy). The $\Upsilon(4S)$ resonance is boosted by $\beta\gamma = 0.425$. There is a 22 mrad crossing angle between the electron and positron beams at the interaction point.

The Belle detector surrounds the beam crossing point. It is a large solid angle spectrometer with a 1.5 T superconducting solenoid magnet. Charged particles are detected by a three layer double-sided silicon vertex detector (SVD) and a 50 layer cylindrical drift chamber (CDC) filled with a helium-ethane gas mixture. The tracking acceptance covers the laboratory polar angle between $\theta = 17°$ and $150°$ (z is along the beam direction), corresponding approximately to 92% of the full solid angle in the center-of-mass (c.m.) frame. The resolutions in impact parameter and momentum are measured to be 55 μm for a 1 GeV/c charged particle and $\sigma_{p_t}/p_t = (0.30/\beta \oplus 0.19 p_t)\%$, where p_t is the transverse momentum in GeV/c. A CsI(Tl) electromagnetic calorimeter (ECL) is located inside the solenoid coil and covers the same solid angle as the charged particle tracking system. It detects electromagnetic showers with a resolution of $\sigma_E/E = (1.3 \oplus 0.07/E \oplus 0.8/E^{1/4})\%$, where E is in GeV.

Charged hadron identification is accomplished by combining the response from an array of 1188 silica aerogel Čerenkov counters (ACC), an array of 128 time-of-flight counters and specific ionization (dE/dx) measurement in the CDC. An iron flux-return yoke outside the solenoid is comprised of 14 layers of 4.7-cm-thick iron plates interleaved with a system of resistive plate counters [Klong and muon detector (KLM)] that are used for muon identification. The Belle detector is described in detail elsewhere [8].

TABLE I. Analyzed decay chains.

Primary mode	Secondary mode(s)
$B^- \to J/\psi \pi^-$	$J/\psi \to l^+ l^-$
$\overline{B}^0 \to J/\psi \pi^0$	$J/\psi \to l^+ l^-$, $\pi^0 \to \gamma\gamma$
$B^- \to J/\psi K^-$	$J/\psi \to l^+ l^-$
$\overline{B}^0 \to J/\psi K_S^0$	$J/\psi \to l^+ l^-$, $K_S^0 \to \pi^+ \pi^-$
$B^- \to \psi(2S) K^-$	$\psi(2S) \to l^+ l^-$, $\psi(2S) \to J/\psi \pi^+ \pi^- \{ J/\psi \to l^+ l^- \}$
$\overline{B}^0 \to \psi(2S) K_S^0$	$\psi(2S) \to l^+ l^-$, $\psi(2S) \to J/\psi \pi^+ \pi^- \{ J/\psi \to l^+ l^- \}$, $K_S^0 \to \pi^+ \pi^-$

III. EVENT SELECTION

Hadronic events are selected by requiring (1) at least three reconstructed charged tracks, (2) a total reconstructed ECL energy in the c.m. in the range 0.1 to 0.8 times the total c.m. energy, (3) at least one large-angle cluster in the ECL, (4) a total visable energy (sum of charged tracks and neutral showers not matched to tracks) greater than 0.2 times the total c.m. energy, (5) absolute value of the z component of the c.m. momentum less than 50% of the total c.m. energy, and (6) a reconstructed primary vertex that is consistent with the known location of the interaction point. These selection criteria are determined by Monte Carlo simulation to be 99% efficient for signal events. To suppress two-jet non-$\Upsilon(4S)$ background relative to $B\overline{B}$ events we require that $R_2 < 0.5$, where R_2 is the ratio of the second to zeroth Fox-Wolfram moments [10]. To remove charged particle tracks that are badly measured or do not come from the interaction region, we require $dz < 5$ cm for all tracks other than those identified as decay daughters of K_S^0, where dz is the absolute value of the coordinate along the beam direction at the point on the track nearest the origin.

The decay modes considered are listed in Table I. (Hereafter the inclusion of the charge conjugate states is implied.)

A. $J/\psi[\psi(2S)]$ candidates

In this analysis, J/ψ candidates are reconstructed from oppositely charged lepton pairs, $\mu^+ \mu^-$ or $e^+ e^-$. Lepton candidates are selected with tight or loose criteria depending on the background level for each mode. For muon tracks, tight identification is based on track penetration depth and hit scatter in the KLM system [11], while loose identification requires that the track have an energy deposit in the ECL that is consistent with that of a minimum ionizing particle. Electron tracks are tightly identified by a combination of dE/dx from the CDC, E/p (E is the energy deposit in the ECL and p is momentum measured by the SVD and the CDC), and shower shape in the ECL [12]. For weak electron identification, either dE/dx or E/p is required to be consistent with the electron hypothesis.

For the identification of J/ψ dilepton decays in the $B \to J/\psi K$ modes we require one tightly and one loosely identified lepton. For the $\psi(2S)K$ and $J/\psi\pi$ modes, both lepton candidates are required to be tightly identified. We correct for final state radiation or bremsstrahlung in the inner parts of the detector by including the four-momentum of every photon detected within 0.05 rad of the original electron or positron direction in the $e^+ e^-$ invariant mass calculation. Figure 1 shows the dilepton mass distribution near the J/ψ mass. The mass resolutions are 9.3 MeV/c^2 and 10.6 MeV/c^2 in the peak region for $\mu^+ \mu^-$ and $e^+ e^-$, respectively. Since there are still small radiative tails, as can be seen in Fig. 1, we use asymmetric invariant mass requirements, $(-60 < m_{\mu^+\mu^-} - m_{J/\psi[\psi(2S)]} < 36)$ MeV/c^2 and $(-150 < m_{e^+e^-} - m_{J/\psi[\psi(2S)]} < 36)$ MeV/c^2, for the $\mu^+ \mu^-$ and $e^+ e^-$ pairs respectively.

To identify $\psi(2S) \to J/\psi \pi^+ \pi^-$ candidates, we combine J/ψ candidates with pairs of oppositely charged tracks that have a $\pi^+ \pi^-$ invariant mass greater than 400 MeV/c^2. The $\psi(2S)$ and J/ψ candidates' mass difference is required to be consistent with the known difference, $(0.58 < m_{l^+l^-\pi^+\pi^-} - m_{l^+l^-} < 0.60)$ GeV/c^2. This range corresponds to $\pm 3\sigma$ in detector resolution. Figure 2 shows (a) the invariant mass distribution of $\psi(2S) \to ll$, and (b) the mass difference of $m_{ll\pi\pi} - m_{ll}$.

B. Light meson candidates

In the analysis for $B^- \to J/\psi[\psi(2S)]K^-$, all charged tracks (other than those used for ψ reconstruction) are used as kaon candidates in order to eliminate the systematic error from particle identification. This does not introduce any serious additional background, because the principal background is expected to be from $B^- \to J/\psi[\psi(2S)]\pi^-$ decays, which occur at a much lower rate than $J/\psi[\psi(2S)]K^-$. The prompt charged pion candidates are conversely required to be strongly identified as pions $[P(\pi/K) > 0.9]$, where the likelihood ratio for a particle to be a charged pion, $P(\pi/K) = \text{Prob}(\pi)/[\text{Prob}(\pi) + \text{Prob}(K)]$, is calculated using dE/dx measured in the CDC and the response of the ACC.

For the analysis of neutral B meson decays, the reconstruction of $K_S^0 \to \pi^+ \pi^-$ is made by selecting pairs of oppositely charged tracks with $\pi^+ \pi^-$ invariant mass between 482 and 514 MeV/c^2. This criterion retains 99.7% of $K_S^0 \to \pi^+ \pi^-$ decays with detected tracks, based on a double Gaussian fit to the mass peak of the data (the average mass resolution is 4.4 MeV/c^2). In order to reduce combinatorial background further, we require the following:

If both pions have associated SVD hits, the points of nearest approach of the two tracks in the projection onto the plane perpendicular to the beam line (r-ϕ) are separated in the beam direction (z) by less than 1 cm.
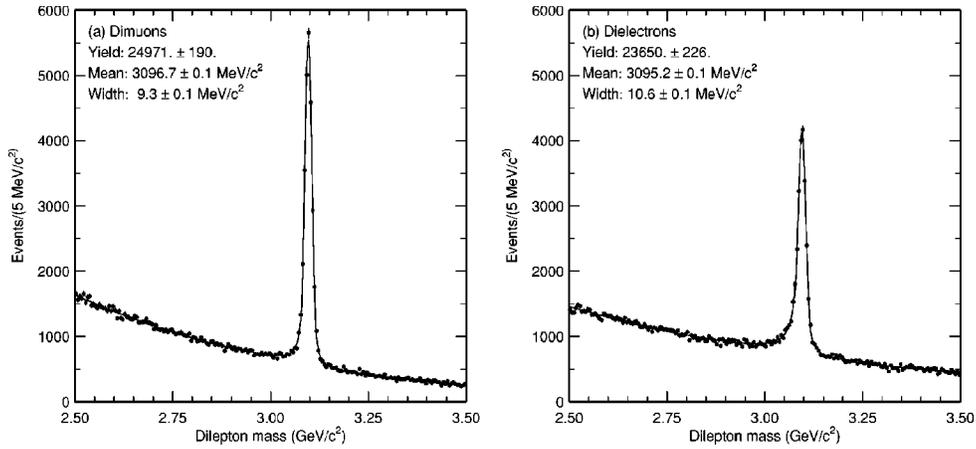
FIG. 1. The invariant mass distributions for (a) $\mu^+\mu^-$ and (b) e^+e^-. In these figures, both leptons are tightly identified.

If only one of the two pions has associated SVD hits, the distance of nearest approach to the interaction point in the r-ϕ projection be greater than 250 μm for both tracks.

If neither of the two pions have associated SVD hits, the ϕ coordinate of the $\pi^+\pi^-$ vertex point and the ϕ direction of the $\pi^+\pi^-$ candidate's three-momentum agree within 0.1 rad.

The K_S^0 identification efficiency after track selection is 95%.

In the selection of $B^0 \rightarrow J/\psi\pi^0$, the high momentum π^0's are reconstructed from pairs of detected photons. The invariant mass is required to be 118 MeV/$c^2 < m_{\gamma\gamma} < 150$ MeV/c^2 (mass resolution is 5.3 MeV/c^2). The π^0 candidate is also to have a good mass constrained fit.

C. B meson reconstruction

B mesons are reconstructed by combining a charmonium meson candidate with a kaon or pion candidate, as described above. The energy difference, $\Delta E \equiv E_{cand} - E_{beam}$, and the beam-energy constrained mass, $M_{bc} \equiv \sqrt{E_{beam}^2 - P_{cand}^2}$, are used to separate signal from background [E_{beam} is the beam energy, E_{cand} and P_{cand} are the B candidate energy and momentum, all calculated in the $\Upsilon(4S)$ center of mass frame].

In this calculation, kinematic fits are performed with (1) mass and vertex constraints for the J/ψ or $\psi(2S)$ di-lepton decays and K_S^0 decays, and (2) a mass constraint for the $\psi(2S) \rightarrow J/\psi\pi^+\pi^-$ and $\pi^0 \rightarrow \gamma\gamma$ decays. Figure 3 shows the distribution for $B \rightarrow J/\psi K^{\pm}$ candidates in the M_{bc}-ΔE plane as well as in ΔE after projecting out candidates with M_{bc} between 5.27 and 5.29 GeV/c^2. In the first plot an excess of candidates is clearly apparent in the signal region, indicated by the rectangle.

In order to determine yields, we fit the M_{bc} distributions after applying the following requirements on ΔE: for all modes except $J/\psi\pi$, $(-40 < \Delta E < 40)$ MeV; for the $J/\psi\pi^0$ decay mode, $(-100 < \Delta E < 50)$ MeV, as the ΔE distribution has a long tail at negative values due to material in the detector and energy leakage; for the $J/\psi\pi^-$ mode, $(-10 < \Delta E < 40)$ MeV, to suppress a background from $B \rightarrow J/\psi K^-$ due to misidentification of K^- as π^-.

The fit of the M_{bc} distribution is performed with the sum of a Gaussian for signal and the ARGUS function [13] for background (Fig. 4). The resolution in M_{bc} is dominated by the energy spread of KEKB. We test the resolution agreement between Monte Carlo (MC) simulated data and real data using the mode $B^- \rightarrow J/\psi K^-$ (which has the highest
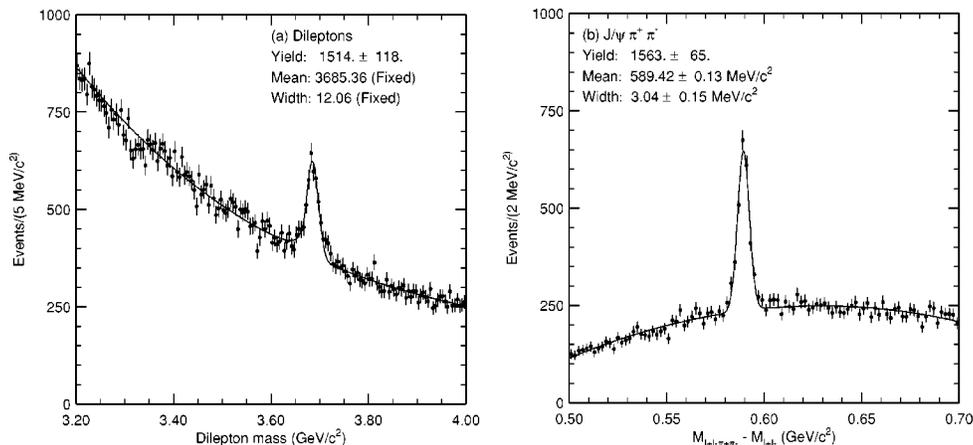
FIG. 2. (a) The invariant mass distribution of $\psi(2S) \rightarrow l^+l^-$ candidates; (b) the mass difference of $m_{l^+l^-\pi^+\pi^-} - m_{l^+l^-}$.
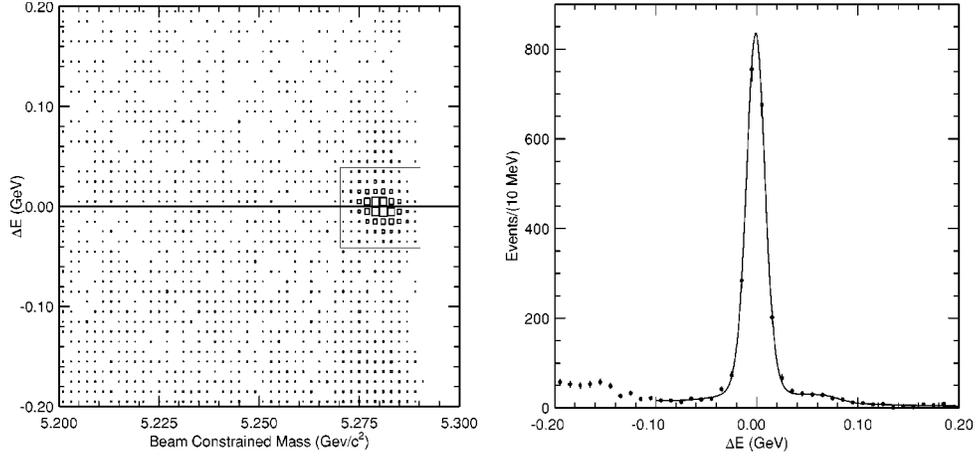
FIG. 3. The distribution of (a) ΔE versus $M_{\rm bc}$ and (b) ΔE for $B \rightarrow J/\psi K^{\pm}$. The background from $B \rightarrow J/\psi K^*$ is seen at lower ΔE, while that from $B \rightarrow J/\psi \pi^{\pm}$ is at higher ΔE.

statistics). The agreement is very good and we use the MC predicted widths for each mode to fit the $M_{\rm bc}$ histograms. The signal yield and the normalization of the background are allowed to vary in the fit. The results are shown in Table II.

For the $J/\psi \pi^-$ mode, as shown in Fig. 5, the background from $B^- \rightarrow J/\psi K^-$ peaks in the signal region of $M_{\rm bc}$ but accumulates near $\Delta E \sim -70$ MeV due to kinematic differences from the signal mode. To ensure that it does not intrude into the signal in the $M_{\rm bc}$ fit, a fit is performed on the ΔE distribution with two separated Gaussians and a first-order Chebyshev polynomial function (Fig. 5). The signal

yield obtained from the ΔE distribution fit is consistent with the $M_{\rm bc}$ fit. The background yield from $J/\psi K^-$ is also consistent with the expectation from the mis-identification probability.

IV. RESULTS

A. Branching fractions

The reconstruction efficiencies are determined by Monte Carlo simulations based on GEANT [7] and are listed in Table II. The number of $B\bar{B}$ events is measured to be (31.9 ± 0.3)
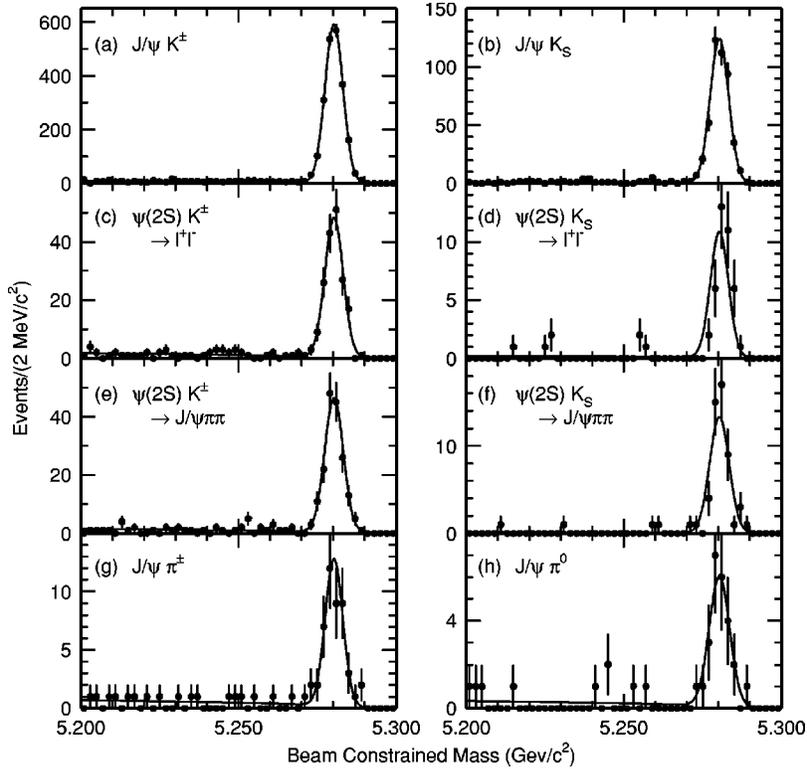
FIG. 4. The distribution of $M_{\rm bc}$ for (a) $B^- \rightarrow J/\psi K^-$, (b) $\bar{B}^0 \rightarrow J/\psi K_S^0$, (c) $B^- \rightarrow \psi(2S)K^-\{\psi(2S) \rightarrow l^+ l^-\}$, (d) $\bar{B}^0 \rightarrow \psi(2S)K_S^0\{\psi(2S) \rightarrow l^+ l^-\}$, (e) $B^- \rightarrow \psi(2S)K^-\{\psi(2S) \rightarrow J/\psi \pi^+ \pi^-\}$, (f) $\bar{B}^0 \rightarrow \psi(2S)K_S^0\{\psi(2S) \rightarrow J/\psi \pi^+ \pi^-\}$, (g) $B^- \rightarrow J/\psi \pi^-$, and (h) $\bar{B}^0 \rightarrow J/\psi \pi^0$.

TABLE II. Signal yields and branching fractions (BF) for each mode. Signal yields are determined by fitting. The errors are statistical (first error) and systematic (second), except for the combined $\psi(2S)$ modes where the total error is listed. Efficiencies for modes with K^0 mesons are for reconstructing $B \to \psi K_S^0$.

Decay mode		Yield	Efficiency(%)	BF ($\times 10^{-4}$)
$B^- \to J/\psi \pi^-$		43.9 ± 6.8	33.3 ± 0.6	$0.38 \pm 0.06 \pm 0.03$
$\overline{B^0} \to J/\psi \pi^0$		24.0 ± 5.0	27.2 ± 0.5	$0.23 \pm 0.05 \pm 0.02$
$B^- \to J/\psi K^-$		2102 ± 46	55.3 ± 0.7	$10.1 \pm 0.2 \pm 0.7$
$\overline{B^0} \to J/\psi K^0$		453 ± 21	30.5 ± 0.6	$7.9 \pm 0.4 \pm 0.9$
$B^- \to \psi(2S) K^-$				6.9 ± 0.6
	$\psi(2S) \to l^+ l^-$	173 ± 13	51.6 ± 0.7	$7.3 \pm 0.6 \pm 0.7$
	$\psi(2S) \to J/\psi \pi^+ \pi^-$	170 ± 13	23.2 ± 0.5	$6.4 \pm 0.5 \pm 0.8$
$\overline{B^0} \to \psi(2S) K^0$				6.7 ± 1.1
	$\psi(2S) \to l^+ l^-$	38.5 ± 6.2	27.5 ± 0.5	$6.1 \pm 1.0 \pm 0.8$
	$\psi(2S) \to J/\psi \pi^+ \pi^-$	51.2 ± 7.2	12.0 ± 0.4	$7.4 \pm 1.0 \pm 1.3$

$\times 10^6$. In the calculation of the branching fraction, the production rates of $B^+ B^-$ and $B^0 \bar{B}^0$ pairs are assumed to be equal. We use the secondary branching fractions listed in Table III [14]. The resulting branching fractions for each reconstructed decay chain are summarized in Table II, where the first errors are statistical and the second are systematic. The measurement values for the two $\psi(2S)$ modes of $B \to \psi(2S)K$ are consistent within their errors and the combined results are also listed in the table (taking into account correlated and uncorrelated errors).

The sources of systematic error are shown in Table IV. The dominant uncertainty arise from the uncertainty in the tracking efficiency.

The tracking efficiency uncertainty is determined to be 2% per track from a comparison of the yields for η

$\to \pi^+ \pi^- \pi^0$ and $\eta \to \gamma\gamma$ with MC expectations. The pion tracks from K_S^0 decay are from a displaced vertex and thus may have a larger systematic error. We include a 3.5% per track uncertainty for these tracks (see below).

The uncertainty in the K_S^0 selection efficiency is checked by comparing yields for a sample of high momentum $K_S^0 \to \pi^+ \pi^-$ decays before and after applying the K_S^0 selection criteria to a sample of K_S^0's in hadronic events. The efficiency difference between data and the Monte Carlo simulation is less than 1.0%.

As one cross-check of K_S^0 reconstruction, we also estimate the difference between data and non-$\Upsilon(4S)$ MC simulated data directly, using the yield ratio between $D^0 \to K_S^0 \pi^+ \pi^-$ and $D^0 \to K^- \pi^+$ with D^0's from $D^* \to D^0 \pi$ decay. In this case, D^0's with momentum higher than 3.0 GeV/c are selected. The difference of the ratio between the data and MC program is also smaller than 1%, where a large systematic error arises from the uncertainties of the world averages for the branching fractions.

The high momentum π^0 efficiency is checked by taking the ratio between $D^0 \to K^+ \pi^- \pi^0$ and $D^0 \to K^+ \pi^-$ with high momentum D^0's. D^0's generated from D^* decay with a slow pion are selected. We assign a 7% uncertainty to the π^0 efficiency.

The efficiency of lepton identification is checked by comparing the J/ψ yield with one lepton tightly identified against the yield where both leptons are tightly identified. We find that the efficiencies for tightly identified electrons and muons
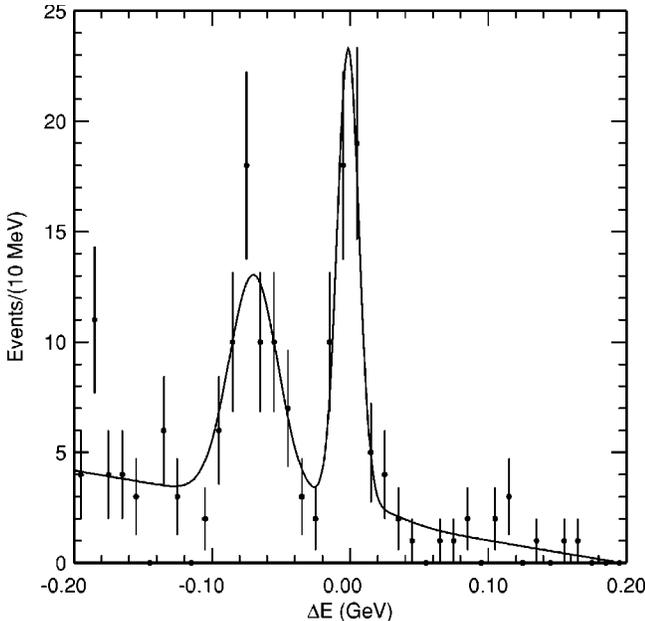
FIG. 5. The ΔE distribution for $B^\pm \to J/\psi \pi^\pm$. The signal peak is seen around zero. The peak at -0.07 GeV/c^2 is from $B^\pm \to J/\psi K^\pm$. In this figure, we require $5.27 < M_{bc} < 5.29$ GeV/c^2.

TABLE III. Branching fractions used for secondary charmonium decays [14].

Decay mode	Branching fraction
$J/\psi \to e^+ e^-$	0.0593 ± 0.0010
$J/\psi \to \mu^+ \mu^-$	0.0588 ± 0.0010
$\psi(2S) \to e^+ e^-$	0.0073 ± 0.0004
$\psi(2S) \to \mu^+ \mu^-$	0.0070 ± 0.0009
$\psi(2S) \to J/\psi \pi^+ \pi^-$	0.305 ± 0.016

TABLE IV. The dominant sources of systematic errors (in %).

Decay mode	Tracking efficiency	Lepton identification efficiency	Hadron identification efficiency	$K_S^0(\pi^0)$ efficiency	Charmonium branching fractions	Monte Carlo statistics	Total
$B^- \to J/\psi \pi^-$	6.0	4.0	2.0		1.2	1.7	7.8
$\overline{B}^0 \to J/\psi \pi^0$	4.0	4.0		7.0	1.2	1.9	9.3
$B^- \to J/\psi K^-$	6.0	2.0			1.2	1.4	6.6
$\overline{B}^0 \to J/\psi K^0$	11.0	2.0		1.0	1.2	1.8	11.4
$B^- \to \psi(2S) K^-$							
$\quad \psi(2S) \to l^+ l^-$	6.0	4.0			5.0	1.4	8.9
$\quad \psi(2S) \to J/\psi \pi^+ \pi^-$	10.0	4.0	4.0		5.3	2.1	12.8
$\overline{B}^0 \to \psi(2S) K^0$							
$\quad \psi(2S) \to l^+ l^-$	11.0	4.0		1.0	5.0	1.9	12.9
$\quad \psi(2S) \to J/\psi \pi^+ \pi^-$	15.0	4.0	4.0	1.0	5.3	2.9	17.1

are 96% and 94%, respectively. The systematic errors from lepton identification are determined to be 2% per tightly identified lepton. The error for loosely identified leptons is negligable.

For the $B^- \to J/\psi \pi^-$ mode, the identification of high momentum charged pions is studied by comparing $D^{*+} \to D^0 \pi^+$, where $D^0 \to K^- \pi^+$, between data and MC simulation. In this decay mode, the D^0 mass peak is reconstructed with small background without any particle identification requirements. The systematic uncertainty is determined by examining the difference in yield before and after applying particle identification. We assign a systematic uncertainty of 2% to the pion identification efficiency.

We also study the systematic error arising from the background in the fit of the M_{bc} distribution. The ARGUS function represents the M_{bc} distribution for the ΔE sidebands well. However there may be background decay modes that peak in the signal region. We checked this with inclusive J/ψ MC simulations and find no evidence for peaking background.

B. Charge asymmetries

The yields for positive and negative B mesons decays are measured separately using the method described above. The charge asymmetries, defined by

$$A_{K(\pi)} = \frac{Br(B^- \to \text{charmonium} + K^-(\pi^-)) - Br(B^+ \to \text{charmonium} + K^+(\pi^+))}{Br(B^- \to \text{charmonium} + K^-(\pi^-)) + Br(B^+ \to \text{charmonium} + K^+(\pi^+))} \tag{1}$$

(see [15]), are calculated assuming the same efficiencies for both charged decays. The results are shown in Table V. The efficiency difference between positive and negative particles is determined by using 3.96×10^5 and 3.33×10^5 events for

$D^\pm \to K^\mp \pi^\pm \pi^\pm$ and $D^0 \to K^- \pi^+ / \overline{D}^0 \to K^+ \pi^-$ decays, respectively. We calculate the efficiency ratios $\epsilon_{\pi^-}/\epsilon_{\pi^+} = 1.011 \pm 0.015$ and $\epsilon_{K^-}/\epsilon_{K^+} = 1.004 \pm 0.017$ using the following formulas:

TABLE V. Charge asymmetry for each mode. Errors are statistical only.

Decay mode	Yield($-$)	Yield($+$)	$A_{K(\pi)}$
$B^\pm \to J/\psi \pi^\pm$	21 ± 5	22 ± 5	-0.023 ± 0.164
$B^\pm \to J/\psi K^\pm$	1024 ± 32	1078 ± 33	-0.026 ± 0.022
$B^\pm \to \psi(2S)(l^+ l^-) K^\pm$	79 ± 9	93 ± 10	-0.081 ± 0.078
$B^\pm \to \psi(2S)(J/\psi \pi^+ \pi^-) K^\pm$	68 ± 8	102 ± 10	-0.200 ± 0.075
Total $(B^\pm \to J/\psi[\psi(2S)] K^\pm)$	1171 ± 34	1273 ± 36	-0.042 ± 0.020

$$\frac{\epsilon_{\pi^-}}{\epsilon_{\pi^+}} = \frac{N(D^- \to K^+ \pi^- \pi^-)N(D^0 \to K^- \pi^+)}{N(D^+ \to K^- \pi^+ \pi^+)N(\overline{D^0} \to K^+ \pi^-)}, \qquad (2)$$

$$\frac{\epsilon_{K^-}}{\epsilon_{K^+}} = \frac{N(D^- \to K^+ \pi^- \pi^-)N(D^0 \to K^- \pi^+)^2}{N(D^+ \to K^- \pi^+ \pi^+)N(\overline{D^0} \to K^+ \pi^-)^2}. \qquad (3)$$

No significant efficiency differences are observed for either pion or kaon tracks. Thus, we do not correct the central values but we do include the error of the efficiency differences in the systematic errors.

Finally, we find the charge asymmetries $-0.023 \pm 0.164 \pm 0.015$ and $-0.042 \pm 0.020 \pm 0.017$ for the charmonium $+\pi$ mode and the charmonium$+K$ mode, respectively. Our results are consistent with zero asymmetry and previous measurements [15,16].

V. CONCLUSION

We have reported measurement of B meson branching fractions to two-body final states that include a J/ψ or $\psi(2S)$ meson and a K_S^0, $K^\pm$, π^0 or $\pi^\pm$. A total of 31.9 million $B\bar{B}$ events accumulated at the $\Upsilon(4S)$ resonance are used for this analysis. Our results are in good agreement with previous measurements [17,18]. Charge asymmetries are also measured and found to be consistent with zero.

[1] BaBar Collaboration, B. Aubert *et al.*, Phys. Rev. Lett. **87**, 091801 (2001).

[2] Belle Collaboration, K. Abe *et al.*, Phys. Rev. Lett. **87**, 091802 (2001).

[3] A.B. Carter and A.I. Sanda, Phys. Rev. D **23**, 1567 (1981); I.I. Bigi and A.I. Sanda, Nucl. Phys. **B193**, 85 (1981).

[4] M. Kobayashi and T. Maskawa, Prog. Theor. Phys. **49**, 652 (1973).

[5] T. Brown, S. Pakvasa, and S.F. Tuan, Phys. Lett. **136B**, 117 (1984); I. Dunietz, Phys. Lett. B **316**, 561 (1993).

[6] G.H. Wu and A. Soni, Phys. Rev. D **62**, 056005 (2000).

[7] R. Brun *et al.*, GEANT 3.21, CERN Report No. DD/EE/84-11, 1987.

[8] Belle Collaboration, K. Abe *et al.*, KEK Progress Report 2000-4, 2000; K. Abe *et al.*, Nucl. Instrum. Methods Phys. Res. A **479**, 117 (2002).

[9] S. Kurokawa *et al.*, KEK Report No. 2001-157, 2001.

[10] G.C. Fox and S. Wolfram, Phys. Rev. Lett. **41**, 1581 (1978).

[11] A. Abashian *et al.*, Nucl. Instrum. Methods Phys. Res. A **491**, 69 (2002).

[12] K. Hanagaki, H. Kakuno, H. Ikeda, T. Iijima, and T. Tsukamoto, Nucl. Instrum. Methods Phys. Res. A **485**, 490 (2002).

[13] ARGUS Collaboration, H. Albrecht *et al.*, Phys. Lett. B **241**, 278 (1990).

[14] Particle Data Group, K. Hagiwara *et al.*, Phys. Rev. D **66**, 010001 (2002).

[15] CLEO Collaboration, G. Bonvicini *et al.*, Phys. Rev. Lett. **84**, 5940 (2000).

[16] BaBar Collaboration, B. Aubert *et al.*, Report No. SLAC-PUB-8942, hep-ex/0108009.

[17] BaBar Collaboration, B. Aubert *et al.*, Phys. Rev. D **65**, 032001 (2002).

[18] CLEO Collaboration, P. Avery *et al.*, Phys. Rev. D **62**, 051101(R) (2000); CLEO Collaboration, S.J. Richichi *et al.*, *ibid.* **63**, 031103(R) (2001).